

Noncoherent Demodulation for Cooperative Diversity in Wireless Systems

Deqiang Chen and J. Nicholas Laneman
Department of Electrical Engineering
University of Notre Dame
Notre Dame, IN 46556
Email: {dchen2, jlaneman}@nd.edu

Abstract—This paper develops a general framework for maximum likelihood (ML) demodulation in cooperative wireless systems with a demodulate-and-forward (DF) protocol at the relays. Although this general structure admits both coherent and noncoherent modulation, we analyze performance of this demodulator mainly for noncoherent demodulation and compare to existing results for coherent demodulation. The ML demodulator consists of a band of square-law devices followed by a nonlinear combiner. We develop an accurate approximation for this demodulator using a band of square-law devices followed by a piecewise-linear (PL) combiner. This approximation not only has certain implementation advantages, but also leads to a tight closed form approximation for the bit error rate (BER) of the ML demodulator. Based on this closed-form result, we derive a high signal-noise-ratio (SNR) approximation, that provides a simpler but tight approximation of the BER of the ML demodulator.

I. INTRODUCTION

Diversity techniques have been widely accepted as one of the effective ways to combat multipath fading in wireless communications [1]. Among other approaches, multiple transmit or receive antennas at the same terminal are often desirable for providing spatial diversity. However, in many scenarios, such as in cellular, ad hoc or sensor networks, multiple antennas can often be precluded due to size limitation of the terminals. Cooperative diversity [2], [3], [4] avoids this size limitation and provides spatial diversity by allowing the terminals to relay in parallel, thus sharing multiple antennas belonging to different terminals.

A. Related Research

In [4], maximum likelihood (ML) demodulators and corresponding analysis, in terms of uncoded bit error rate (BER), are developed for coherent cooperative diversity. It is also pointed out that systems with an amplifying relay appear to perform comparably, if not better, than systems with a demodulating relay. This fact, in addition to the relative simplicity of amplify-and-forward (AF), has led to further analysis of AF in [5], [6]. Using a moment-generating function method, [5] proposes a “blind” relay that does not require instantaneous channel state information (CSI) between the source and relay, but this introduces instantaneous power saturation. Building upon methods from [7], [6] provides closed-form approximations of average symbol error probability (SEP) for general, multi-branch, multi-hop cooperative

diversity transmission schemes for asymptotically high signal-noise-ratio (SNR). It also demonstrates that, in the sense of minimizing SEP for sufficiently high SNR, it is best for the relay to be halfway between the source and destination.

All of these previous works assume that the destination, and possibly the relay, accurately estimates the fading coefficients along the corresponding paths. In slow-fading scenarios [8], such CSI might be obtained by estimation from training sequences in the protocol headers. However, in fast fading scenarios, CSI may not be accurately obtainable if the fading coefficients vary quickly within the period of one transmission block. Also, as the coherence time decreases, estimation of CSI reduces effective transmission rate substantially since pilot tones must be inserted. In these scenarios, noncoherent modulation and demodulation can be more practical. In addition, noncoherent modulation and demodulation are robust methods for realizing control signaling in wireless networks. To the best of our knowledge, there has not been a comprehensive treatment of noncoherent demodulation for cooperative communication schemes. This has been the motivation for our work.

B. Summary of Results

In the following sections, we develop:

- 1) A general framework for ML demodulation of both coherent and noncoherent cooperative diversity schemes, focusing mainly on the noncoherent case.
- 2) A demodulator with a piecewise-linear (PL) combiner that closely approximates the ML demodulator for demodulate-and-forward (DF).
- 3) A closed-form expression for the uncoded BER of the demodulator based on the PL combiner. Numerical results show that this expression provides a tight approximation of the performance of the nonlinear ML demodulator for all SNR regions we simulated.
- 4) Based on this closed-form BER, we derive a high SNR approximation which shows the diversity order of cooperative diversity with noncoherent DF.

II. SYSTEM MODEL

As shown in Fig. 1, the *source* terminal broadcasts the signal x_0 to the *relays* and *destination* in the first subchannel. The relays, denoted as R_i , $i = 1, \dots, M - 1$, and destination

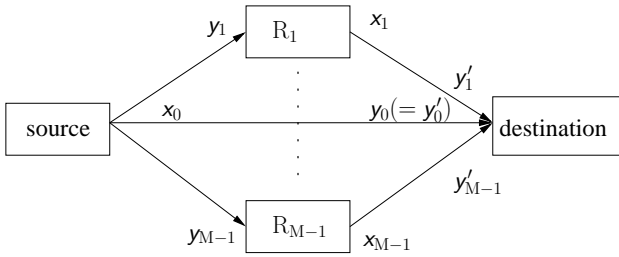


Fig. 1. Block diagram for cooperative diversity with multiple relays.

receive y_i and y_0 , respectively. After some processing, the relays retransmit signals to the destination in the remaining $M - 1$ orthogonal subchannels. The orthogonal subchannels can be realized by CDMA [2], [3], TDMA, FDMA [4], etc. These methods generally increase the requirement of bandwidth in cooperative diversity. Space-time coding [9] can be employed to increase the bandwidth efficiency. For simplicity of exposition, this paper only focuses on a simple TDMA scheme to realize the orthogonality condition.

In [4], two possible signal processing schemes at the relay, namely amplify-and-forward (AF) and demodulate-and-forward (DF), are suggested. Both protocols are comparable in performance in the context of coherent demodulation. The AF protocol appears to be easier to implement as the relays simply amplify and transmit the signal received from the source without forming an estimate of the transmitted signal. However, in noncoherent scenarios, instantaneous power saturation can occur because the relays lack CSI [5]. In DF, the relays demodulate and retransmit the source signal and thereby avoid power saturation. In addition, DF provides more flexibility for a variety of post-processing methods at the relay if it is not limited to symbol-by-symbol retransmission and channel coding is employed [10], [11], [12]. Thus, to ensure a power constraint at relay with potential coding applications in mind, we focus on the uncoded DF protocol in the remainder of the paper.

Overall, the destination receives signals y_0, y'_i from M orthogonal channels. To make the notation more compact, we also define $y'_0 = y_0$. After passing these signals through the appropriate matched filters, we obtain a baseband-equivalent discrete-time model. We focus throughout the paper on binary frequency-shift keying (BFSK) for simplicity of exposition. For BFSK signaling, the outputs from the matched filters can be modeled as

$$\begin{aligned} y'_{i1} &= \frac{x_i + 1}{2} \sqrt{E_i} a_{i,M} + n_{i1}, \\ y'_{i2} &= \frac{1 - x_i}{2} \sqrt{E_i} a_{i,M} + n_{i2}, \end{aligned} \quad (1)$$

where x_i is the sequence from transceiver i and takes values ± 1 , E_i is the average sample energy of the source and relays, $a_{i,j}$ represents the fading coefficient of the corresponding path between transceiver i and j , and n_{i1} and n_{i2} are AWGN. The second subscript 1, 2 in y'_{i1}, y'_{i2} denotes the frequency band.

The fading coefficients $a_{i,j}$ are modeled as zero mean,

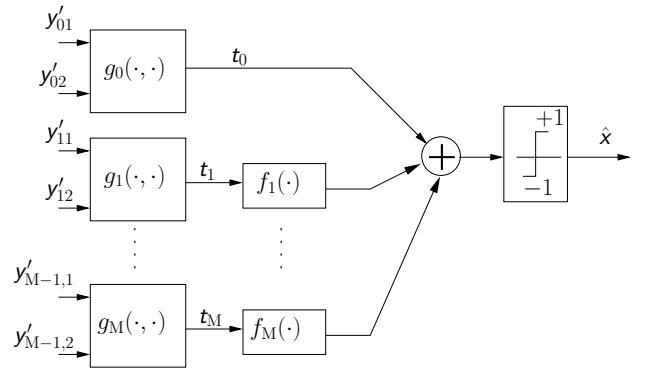


Fig. 2. General demodulator structure for cooperative diversity with multiple relays.

circularly symmetric mutually independent complex Gaussian random variables with variances $\sigma_{a_{i,j}}^2$, and the additive noise $n_{i,j}$ is modeled as zero mean, mutually independent, white complex Gaussian random variables with variance N_0 . The average SNR is defined as $\bar{\gamma}_{i,j} \triangleq \sigma_{a_{i,j}}^2 E_i / N_0$.

III. DEMODULATION ALGORITHMS AND PERFORMANCE

A. Maximum Likelihood Demodulator

The ML demodulator will be implemented as shown in Fig 2. This demodulator structure extends immediately to all coherent and noncoherent binary modulation formats by properly defining functions $g_i(y'_{i1}, y'_{i2}), f_i(t_i)$. Thus, it provides a unified framework for analysis. It might facilitate changes of demodulators according to different transmission formats.

The noise in the orthogonal channels is independent, so the destination observations are conditionally independent given the transmitted signal. Based on this fact, the ML demodulator for the noncoherent cooperative diversity system can be shown to employ the functions

$$g_i(y'_{i1}, y'_{i2}) = \frac{E_i \sigma_{a_{i,2}}^2}{(E_i \sigma_{a_{i,2}}^2 + N_0) N_0} (|y'_{i1}|^2 - |y'_{i2}|^2) \quad (2)$$

for $i = 0, 1$, and

$$f_i(t_i) = \ln \frac{(1 - \epsilon_i) e^{t_i} + \epsilon_i}{\epsilon_i e^{t_i} + (1 - \epsilon_i)}, \quad (3)$$

where ϵ_i is the average probability of error at the relay R_i , which uses a conventional envelope demodulator. The analysis of diversity transmission must treat the nonlinear behavior of (3), which significantly complicates a closed form solution for the probability of error at the destination. As noted in [4], $f_i(t_i)$ essentially “clips” to the values of $\pm \ln[\epsilon_i / (1 - \epsilon_i)]$ for large inputs, and is approximately linear between these extreme values for small inputs. Thus in the sequel we develop a PL approximation to $f_i(t_i)$. This approximation suggests an alternative demodulator, which might be more amenable to practical implementation. Furthermore, as we will see, the performance of the demodulator with PL approximation provides a tight upper bound on the error probability of the ML demodulator.

Finally, we note that, if coherent signaling is employed, we can apply functions

$$g_i(y'_{i1}, y'_{i2}) = \frac{2 (\operatorname{Re}\{y'_{i1} a_{i,2}^*\} - \operatorname{Re}\{y'_{i2} a_{i,2}^*\}) \sqrt{E_i}}{N_0} \quad (4)$$

for $i = 0, 1$, and $f_i(t_i)$ as in (3). In that case, our general demodulator structure can be simplified to the demodulator structure in [4].

An interpretation of this demodulator structure from detection and estimation theory is as follows. The matched filter outputs are processed by a function $g_i(r_1, r_2)$ to produce sufficient statistics. Taking a sufficient statistic as input, the function $f_i(t)$ essentially clips its input using the statistical knowledge of the transmission link. Although this ML demodulator can be applied to the case of multiple parallel relays [13], we focus in the sequel on the case of one relay due to space limitations.

B. Demodulator With PL Combiner

Assuming $\epsilon_1 < 1/2$, our PL combiner is obtained from the following approximation:

$$f_1(t) \cong f_{PL}(t) = \begin{cases} -T_a & \text{for } t \leq -T_a \\ t & \text{for } -T_a \leq t \leq T_a \\ T_a & \text{for } t \geq T_a \end{cases}, \quad (5)$$

where $T_a = \ln[(1 - \epsilon_1)/(\epsilon_1)]$. We note that the diversity combiner resulting from this piecewise-linear approximation relates to the clipped-linear combiners in [14], where the basic idea is to limit the impact of partial-band interference by clipping the output of envelope demodulators with respect to the signal output voltage. In our scenario, we limit the impact of uncertainty in the decisions at the relay. Since the demodulator in [14] employs knowledge of the probability with which the interference appears, our approximations might provide a mechanism for optimizing the clipping level in that context as well.

Now the new demodulator is

$$t_0 + f_{PL}(t_1) \stackrel{\pm 1}{\gtrless} 0, \quad (6)$$

where t_0 and t_1 are the outputs of $g_0(y'_{01}, y'_{02})$ and $g_1(y'_{11}, y'_{12})$ from (2).

Note that conditioned on $x_0 = +1$, t_0 is the difference between two exponential random variables with rates λ_0 and λ'_0 , and t_1 is the difference between two exponential random variables with rates λ_1 and λ'_1 , where

$$\begin{aligned} \lambda_0 &= \frac{1}{\bar{\gamma}_{0,2}}, & \lambda'_0 &= 1 + \frac{1}{\bar{\gamma}_{0,2}}, \\ \lambda_1 &= \frac{1}{\bar{\gamma}_{1,2}}, & \lambda'_1 &= 1 + \frac{1}{\bar{\gamma}_{1,2}}. \end{aligned} \quad (7)$$

Moreover, t_0 and t_1 are conditionally independent given x_0 . Thus, after determining the probability density functions (pdf)

of these two random variables, by applying the total probability law to (6) and performing the integration, we obtain the involved, but closed-form, expression for BER

$$\begin{aligned} P_b &= h(\lambda'_0, \lambda_0, -T_a) \times \{(1 - \epsilon_1)[1 - h(\lambda'_1, \lambda_1, T_a)] \\ &\quad + \epsilon_1 [1 - h(\lambda_1, \lambda'_1, T_a)]\} + h(\lambda'_0, \lambda_0, T_a) \times \\ &\quad [(1 - \epsilon_1)h(\lambda'_1, \lambda_1, -T_a) + \epsilon_1 h(\lambda_1, \lambda'_1, -T_a)] \\ &\quad + p(\lambda'_0, \lambda_0, \lambda'_1, \lambda_1, -T_a) \times [h(\lambda'_1, \lambda_1, 0) - h(\lambda'_1, \lambda_1, -T_a)] \\ &\quad \times (1 - \epsilon_1) + p(\lambda'_0, \lambda_0, \lambda_1, \lambda'_1, -T_a) \times [h(\lambda_1, \lambda'_1, 0) \\ &\quad - h(\lambda_1, \lambda'_1, -T_a)] \times \epsilon_1 + q(\lambda'_0, \lambda_0, \lambda'_1, \lambda_1, T_a) \times \\ &\quad [h(\lambda'_1, \lambda_1, T_a) - h(\lambda'_1, \lambda_1, 0)] \times (1 - \epsilon_1) + q(\lambda'_0, \lambda_0, \lambda_1, \lambda'_1, T_a) \\ &\quad \times [h(\lambda_1, \lambda'_1, T_a) - h(\lambda_1, \lambda'_1, 0)] \times \epsilon_1, \end{aligned} \quad (8)$$

where

$$h(r_0, r_1, t) = \begin{cases} 1 - \frac{r_0}{r_0 + r_1} e^{-r_1 t} & \text{for } t \geq 0 \\ \frac{r_1}{r_0 + r_1} e^{r_0 t} & \text{for } t \leq 0 \end{cases}, \quad (9)$$

$$p(r_1, r_2, r_3, r_4, t) = 1 - \frac{r_1 r_3}{(r_1 + r_2)(r_2 + r_3)} \cdot \frac{1 - e^{-(r_2 + r_3)t}}{1 - e^{r_3 t}}, \quad (10)$$

$$q(r_1, r_2, r_3, r_4, t) = \frac{r_2 r_4}{(r_1 + r_2)(r_1 + r_4)} \cdot \frac{1 - e^{-(r_1 + r_4)t}}{1 - e^{-r_4 t}}. \quad (11)$$

We note that $h(r_0, r_1, t)$ is actually the probability distribution function of the difference between two exponential random variables with parameters r_0 and r_1 , respectively.

As we will see in the sequel, this BER expression (8) of the demodulator with the PL combiner provides a tight upper bound on the error probability of the ML demodulator in all cases we consider. This observation suggests that we can use the much simpler (5) rather than the more complex (2) in the demodulator while maintaining the benefit of diversity. We have extended this technique to the case in which the system has two parallel relays [15]. The PL combiner is also applicable to the coherent case, and similar tight performance between this approximation and the ML demodulator are expected.

C. High SNR Approximation

Although (8) provides a close approximation to the performance of cooperative diversity with noncoherent DF, it is too complicated to provide more insights about the system. Therefore, we develop another approximation suitable for high SNR.

Examining (8), we note that three SNRs, namely $\bar{\gamma}_{0,2}$, $\bar{\gamma}_{0,1}$, $\bar{\gamma}_{1,2}$, parameterize performance. Our high SNR approximation allows all three parameters to become large, but keeps them in fixed proportions to one another. This constraint of proportionality serves the purpose of accounting for the effect of network geometry on performance. Specifically, we assume

$$\bar{\gamma}_{0,2} = k_1 \bar{\gamma}, \quad \bar{\gamma}_{0,1} = k_2 \bar{\gamma}, \quad \bar{\gamma}_{1,2} = k_3 \bar{\gamma}, \quad (12)$$

where $\bar{\gamma}$ can be the average SNR and k_1, k_2, k_3 are constants related with the geometry of networks.

The following procedure describes how we obtain the high SNR approximation: substitute (12) into (8) and express the result as a function of $1/\bar{\gamma}$, expand this function in a power series around the point $1/\bar{\gamma} = 0$ by using $(c_2r + c_3)^{1/(c_1r)} \approx 1 - \ln(c_2r)/c_1r$, and drop all but the first term of the series. The result is

$$P_b \approx \frac{1}{\bar{\gamma}^2} \left(\frac{3}{k_1 k_3} + \frac{2 - \ln \frac{1}{k_2} + \ln \bar{\gamma}}{k_1 k_2} \right). \quad (13)$$

As we will see, (13) provides a very tight approximation to the simulation results as SNR becomes large.

If the diversity order is defined as

$$d = \sup\{d : \lim_{\bar{\gamma} \rightarrow \infty} P_b \bar{\gamma}^d < \infty\}, \quad (14)$$

according to (13), the diversity order for cooperative diversity with noncoherent DF is 2. It is shown in [6] that BER of cooperative diversity with coherent AF relay is $P'_b \approx 1/[\bar{\gamma}^2 k_1(k_2 + k_3)]$. Thus cooperative diversity with coherent AF also has diversity order of 2. However, we emphasize here that, although both protocols have the same diversity order, a subtle difference exists as to whether this diversity order is realizable or not since it can be easily observed that

$$\lim_{\bar{\gamma} \rightarrow \infty} P_b \bar{\gamma}^2 = \infty, \quad \lim_{\bar{\gamma} \rightarrow \infty} P'_b \bar{\gamma}^2 = 1/[k_1(k_2 + k_3)]. \quad (15)$$

Moreover, for the multiple-relay case, these two protocols do not have the same diversity order. In [13], it is shown that DF essentially loses half the diversity order of AF.

If we assume k_1, k_2, k_3 are proportional to the distance between terminals, a geometric interpretation of (13) shows that there exists an asymmetry in noncoherent cooperative diversity. The optimum location of the relay for noncoherent DF to achieve the lowest BER depends on SNR values. On the contrary, coherent AF cooperative diversity [6] achieves best performance when the relay is located in the midpoint between the source and destination. However, numerical optimization of (13) suggests that for most practical SNR values, the performance of the DF system is close to optimum when the relay is at the midpoint between the source and destination.

IV. NUMERICAL RESULTS

To verify the accuracy of (8) and (13), numerical results are provided in Figs. 3–5 to show simulated average BER of uncoded BFSK transmissions for relay locations (0.1, 0), (0.5, 0), and (0.9, 0), respectively. The simulation conditions follow the same lines as in [4]. Specifically, the coordinates of the whole communication network are normalized by the distance $d_{0,2}$ between the source and destination transceivers and the positive direction is defined as from source to destination. Without loss of generality, the source is assumed to be located at (0, 0), and the destination located at (1, 0). For simplicity of exposition, the relay is assumed to be located at (l , 0). In general, the coordinates of the relay can be arbitrary. The fading variances $\sigma_{a_{i,j}}^2$ are assigned using a path-loss model in

the form of $\sigma_{a_{i,j}}^2 \propto d_{i,j}^{-v}$, where $d_{i,j}$ is the distance from node i to node j , and v is constant value, chosen to be 4 in our setup. The total network energy per transmitted bit is also normalized to 1. Specifically, we set $E_0 = 1$ for single-hop transmission, and for diversity transmission, we assign equal sharing of power among the transmitters, *i.e.*, $E_0 = E_1 = 1/2$. We note that this power allocation does not consider the channel condition and need not be optimal in general.

Figs. 3–5 show that there is an apparent decrease in slope on a log scale for cooperative diversity transmission in all three cases compared with that of single-hop transmission. This reflects the diversity order gain of cooperative diversity. Furthermore, in Figs. 3–5, the curves for cooperative diversity transmission also demonstrate certain shifts to the left, which combat path-loss. These “coding gains” vary depending on the location of the relay. As suggested in Section III-C, among the three cases we simulated, the highest gain is obtained when the relay is located at the midpoint between the source and destination.

The closed-form BER of the demodulator with PL combiner (8) is also presented in the plots. Its curves essentially overlap the simulation results for the ML demodulator. Since this BER is in closed form and consists of only elementary functions, it is convenient for estimating performance of the ML demodulator, rather than resorting to expensive Monte-Carlo simulations.

The curve for the high SNR approximation (13) are also presented in the plots. Note that $k_1 = 1/2$, $k_2 = d_{0,1}^{-4}/2$, $k_3 = d_{1,2}^{-4}/2$ according to the path-model, and $\bar{\gamma}$ is the average SNR for single hop transmission. In all scenarios, (13) overlaps with simulation results in the regime of high SNR.

Finally, simulation results for the average BER for cooperative diversity with coherent BFSK and BPSK are also displayed in the plots. The shifts among the curves vary slightly with the position of the relay, though, in general, coherent BFSK is about 3 dB worse than BPSK, and about 3 dB better than noncoherent BFSK. Note that, at present, we have no closed-form expression for the error probability of coherent BFSK or BPSK; our results suggest that the approximation (8), plus a suitable shift of 3 dB or 6 dB, provides a good approximation for the performance of these two uncoded schemes.

V. CONCLUSION

This paper discusses noncoherent demodulation for cooperative diversity with DF relays. A piecewise-linear combiner is proposed to approximate the nonlinear ML combiner. This approximation not only reduces complexity in implementation, but also leads to a closed-form expression for BER. Numerical simulations show that this expression provides a very tight upper bound of the performance of ML demodulators in all SNR regimes we simulated. Moreover, a simpler high SNR approximation can be obtained from this closed-form expression, and it is shown to be tight in high SNR regimes.

Although the discussion here is limited to BFSK, with suitable modification, the ML demodulator structure and the

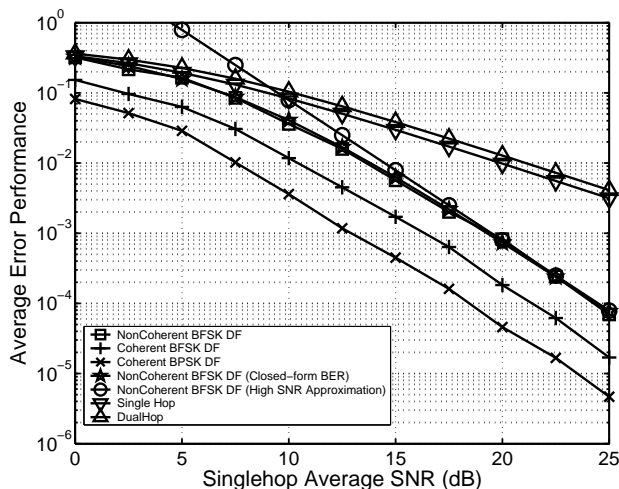


Fig. 3. Error probability performance of the demodulating relay protocols for $v = 4$ and normalized geometries with the relay located at $(0.1,0)$, i.e., close to the source.

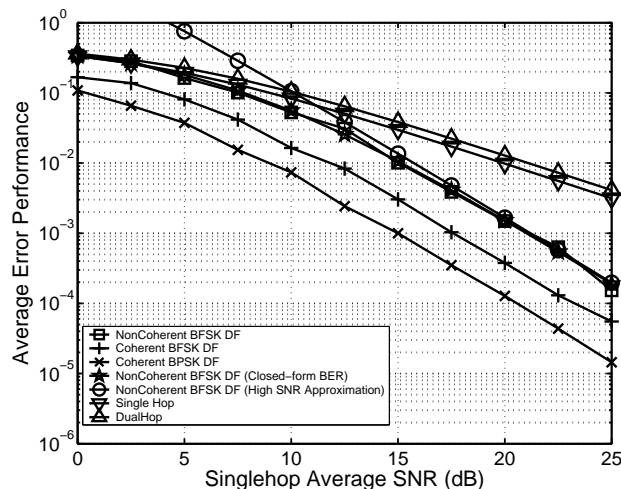


Fig. 5. Error probability performance of the demodulating relay protocols for $v = 4$ and normalized geometries with the relay located at $(0.9,0)$, i.e., close to the destination.

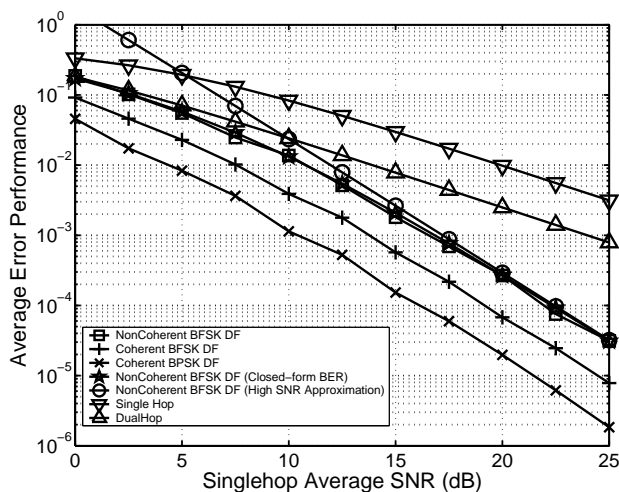


Fig. 4. Error probability performance of the demodulating relay protocols for $v = 4$ and normalized geometries with the relay located at $(0.5,0)$, i.e., halfway between source and destination.

PL combiner can apply to some other orthogonal modulation formats as well, such as multiple-frequency-shift-keying (MFSK) and pulse-position-modulation (PPM). For example, the demodulation of MFSK can be realized by a sequence of binary tests, and the closed form BER developed for BFSK can also be used as part of a union bound for performance of noncoherent MFSK. On the other hand, for differential-phase-shift-keying (DPSK), ML demodulation at the destination becomes more involved due to the error propagation at the relay, and does not fit in the framework we propose here.

ACKNOWLEDGMENT

This work has been supported in part by the State of Indiana through the 21st Century Fund and NSF through grant no. ECS03-29766.

REFERENCES

- [1] J. G. Proakis, *Digital Communications*. McGraw-Hill, Inc., 1995.
- [2] A. Sendonaris, E. Erkip, and B. Aazhang, "User cooperation diversity, Part I: System description," *IEEE Transaction On Communications*, vol. 51, no. 11, pp. 1927–1938, 2003.
- [3] —, "User cooperation diversity, Part II: Implementation aspects and performance analysis," *IEEE Transaction On Communications*, vol. 51, no. 11, pp. 1939–1948, 2003.
- [4] J. N. Laneman and G. W. Wornell, "Energy-efficient antenna-sharing and relaying for wireless networks," in *Proc. IEEE Wireless Communications and Networking Conference (WCNC)*, 2000.
- [5] M. O. Hasna and M.-S. Alouini, "A performance study of dual-hop transmissions with fixed gain relays," in *IEEE International Conference on Acoustics, Speech, and Signal Processing (ICASSP)*, vol. 4, 2003, pp. IV-189–92.
- [6] A. Ribeiro, X. Cai, and G. B. Giannakis, "Symbol error probabilities for general cooperative links," *IEEE Transaction On Wireless Communications*. To Appear, 2004.
- [7] Z. Wang and G. B. Giannakis, "A simple and general parameterization quantifying performance in fading channels," *IEEE Transaction On Communications*, vol. 51, no. 8, pp. 1389–1398, 2003.
- [8] T. S. Rappaport, *Wireless Communications: Principles and Practice*. Prentice-Hall, Inc., 1996.
- [9] J. N. Laneman and G. W. Wornell, "Distributed space-time coded protocols for exploiting cooperative diversity in wireless networks," *IEEE Transaction On Information Theory*, vol. 59, no. 10, 2003.
- [10] M. Janani, A. Hedayat, T. E. Hunter, and A. Nersisyan, "Coded cooperation in wireless communications: Space-time transmission and iterative decoding," *IEEE Transaction On Signal Processing*, to appear.
- [11] A. Stefanov and E. Erkip, "On the performance analysis of cooperative spacetime coded system," in *IEEE Wireless Communications and Networking Conference (WCNC)*, 2003.
- [12] —, "Cooperative space-time coding for wireless networks," in *Proceedings of IEEE Information Theory Workshop*, 2003.
- [13] D. Chen and J. N. Lanema, "Modulation and demodulation for cooperative diversity in wireless systems," *IEEE Transaction On Wireless Communications*, Submitted for publication, 2004.
- [14] C. M. Keller and M. B. Pursley, "Clipped diversity combining for channels with parital-band interference—Part I: Clipped-linear combining," *IEEE Transactions on Communications*, vol. 35, no. 12, 1987.
- [15] D. Chen, "Noncoherent communication theory for cooperative diversity in wireless networks," Master's thesis, University of Notre Dame, 2004.